

Stratified Multivariate Multiscale Dispersion Entropy for Physiological Signal Analysis

Evangelos Kafantaris, Tsz-Yan Milly Lo, Javier Escudero

Abstract—Multivariate Entropy quantification algorithms are becoming a prominent tool for the extraction of information from multi-channel physiological time-series. However, during the analysis of physiological signals from heterogeneous organ systems, certain channels may overshadow the patterns of others, resulting in information loss. Here, we introduce the framework of Stratified Entropy to control the prioritization of each channels' dynamics based on their allocation to respective strata, leading to a richer description of the multi-channel signal. As an implementation of the framework, three algorithmic variations of the Stratified Multivariate Multiscale Dispersion Entropy are introduced. These variations and the original algorithm are applied to synthetic and physiological time-series, formulated from electroencephalogram, arterial blood pressure, electrocardiogram, and nasal respiratory signals. The results of experiments conducted on synthetic time-series indicate that the variations successfully prioritize channels based on their strata allocation while maintaining the low computation time of the original algorithm. Based on the physiological time-series results, the distributions of features extracted from healthy sleep versus sleep with obstructive sleep apnea display increased statistical difference for certain strata allocations in the variations. This suggests improved physiological state monitoring by the variations. Furthermore, stratified algorithms can be modified to utilize a priori knowledge for the stratification of channels. Thus, our research provides a novel approach of multivariate analysis for the extraction of previously inaccessible information from heterogeneous systems.

I. INTRODUCTION

INCREASED amounts of physiological data are becoming available due to the advancement and deployment of physiological recording technology across a range of applications from wearable devices to clinical environments [1]–[3]. The analysis of these data can contribute to effective prognosis, early stage intervention, personalised treatments, and improved clinical decision making. However, for the successful development of algorithms capable of extracting viable information,

certain characteristics of the data have to be considered. These include their multivariate nature due to the interaction of multiple organ systems in human physiology [4]–[8], the potential non-linear nature of their dynamics [9]–[14], and the low data-quality arising from the recording conditions [15]–[17].

Entropy quantification algorithms are becoming a prominent tool for the measurement of dynamics from uni and multi-channel time-series [18]. These algorithms are based on Shannon entropy [19] or on Conditional Entropy defined as the quantity of information observed in a sample at a time-point n that cannot be explained based on previous samples up to time point $n - 1$ [20]. Their implementation has been successful in a variety of applications such as the monitoring of machine operation [21], [22] and the analysis of financial time-series [23], [24].

The use of entropy in the analysis of physiological signals has been extensive. Examples include the utilization of algorithms based on Shannon Entropy such as Permutation Entropy (PEn) [25] and Dispersion Entropy (DisEn) [26], [27] for the analysis of electroencephalogram (EEG) signals to track the state of consciousness of patients while under the effect of anaesthetic drugs [28] and for the analysis of blood pressure signals to quantify the effect of aging in the reduction of the recorded signal's variability [26], respectively. Additionally, algorithms based on conditional entropy have also been utilized, such as Approximate Entropy (ApEn) [29] for the investigation of abnormalities in respiratory function caused by panic disorders [30], Sample Entropy (SampEn) [31] for the analysis of neonatal heart rate variability for diagnosing sepsis [32], and Fuzzy Entropy (FuzzyEn) on surface electromyography (EMG) signals for the detection of motion [33].

For the effective analysis of physiological dynamics multi-channel time-series have to be analyzed both in a univariate and a multivariate manner. This is a necessary step to ensure that, during the analysis of multi-channel time-series, cross-channel dynamics can be quantified, to allow the study of dynamics developed across different components of the same organ system as well as across distinct organ systems [4]–[8]. For this reason, recent research has focused on producing multivariate variations of the aforementioned algorithms: DisEn [34], PEn [35], ApEn, SampEn [36], and FuzzyEn [37] allowing the extraction of features from two or more channels.

However, while the multivariate algorithms are capable of extracting an output feature from a multi-channel time-series, the approach is limited with regards to the total information

Evangelos Kafantaris has a PhD studentship funded by the Engineering and Physical Sciences Research Council, the National Health Service of the United Kingdom, and the Network of European Funding for Neuroscience Research, which is part of the European Research Area Networks.

E. Kafantaris and J. Escudero are with the School of Engineering, Institute for Digital Communications, University of Edinburgh, Edinburgh EH9 3FB, UK. * Corresponding author, email: evangelos.kafantaris@ed.ac.uk

T.Y. Milly Lo is with the Centre of Medical Informatics, Usher Institute, University of Edinburgh EH16 4UX, UK and Royal Hospital for Children & Young Person, Edinburgh EH16 4TJ, UK.

that can be extracted. The dynamics of certain input channels may overshadow those of others due to the potentially different dominant frequencies amongst the physiological signals formulating each channel. This can become particularly apparent when multi-channel time-series are comprised of signals that arise from heterogeneous organ systems such as the combination of electrocardiograms (ECG) [38], EEG [39], arterial blood pressure (BP) [40] and nasal respiratory (RESP) signals [41], [42] whose dominant frequencies and temporal structures display clear differences.

As a step towards addressing this challenge, recent studies have suggested the utilization of non-uniform multiscale embedding between the input channels. This approach aims to find the optimal combination of scales for the analysis of the multi-channel time-series with the aim of utilizing each channel at the scale where most of its dynamics would arise. While this approach offers an interesting and modular configuration of analysis for multi-channel time-series, assuming that an optimal combination of scales is successfully determined, it faces multiple challenges that limit the range of its applicability. These are the potential mismatch of each channel's data length with the optimal scale values, the limitation of multiscale analysis to specific scales for each channel resulting in an incomplete multiscale output, [43], the instability of the method for increased number of channels [44] and the potential for overshadowing to occur even at optimal scale combinations.

A different approach for the analysis of interdependencies within a group of multi-channel time-series arises from the utilization of Cross-Entropy algorithms, which have been developed for ApEn, SampEn [31], FuzzyEn [45] and PEn [46]. With them, an entropy based feature quantifies the coupling between two channels (A) and (B). The variations of SampEn and FuzzyEn are non-directional, the output value of measuring the coupling of A to B would be equal to that of B to A . In contrast, the variations of ApEn and PEn are directional and therefore one of the two channels acts as the designated channel in the measurement. In this form of bivariate analysis, the potential overshadowing of each channels' dynamics could be avoided, particularly when considering the directionality of the ApEn and PEn variations since in their implementation each channel has the opportunity to be in the designated position. However, this approach is limited to bivariate measurements between sets of two channels and therefore would not be able to capture higher-order dynamics that would arise from combining three or more channels. A second limitation is that, by definition, the extracted value measures the coupling between the two channels and is not a measurement of their combined dynamics.

In this study, we propose the framework of Stratified-Entropy that aims to combine positive elements of both the Multivariate and Cross-Entropy category of algorithms to augment the information that can be extracted from a set of multi-channel time-series by allowing each channel's dynamics to be in a different level of prioritization during quantification of the output entropy value based on its allocation to a respective stratum. Consequently, the main contributions of the presented work are:

- The introduction of Stratified-Entropy framework for multivariate and multiscale analysis.
- The implementation of the Stratified-Entropy framework through the introduction of three novel algorithms of Stratified Multivariate Multiscale Dispersion Entropy (SmvMDE).
- The analysis and benchmarking of the operation of the SmvMDE algorithms through experiments applied to both synthetic and physiological time-series.

II. METHODS

A. Stratified Entropy Framework

Within the framework of Stratified Entropy, strata are defined with a clear hierarchy of prioritization. The number of strata can vary based on the implementation of the framework. In the first stage of Stratified Entropy analysis, each channel is allocated to one of the available strata. During the entropy quantification process, the channels have a weighted contribution in the calculation of the output entropy feature based on their allocated stratum.

We build upon the existing mvMDE algorithm and introduce three novel variations of the Stratified Multiscale Multivariate Dispersion Entropy algorithm (SmvMDE). These are: The Threshold (T-SmvMDE), Soft Threshold (ST-SmvMDE) and Proportional (P-SmvMDE) variations.

For the purposes of this study all three variations have been designed based on a two strata configuration, a core stratum (prioritized) and a periphery stratum. The potential extension to configurations with higher numbers of strata is discussed in subsection III-D.3. The variations differ with regards to the algorithmic operations used for the prioritization of the dynamics of channels allocated to the core stratum over the periphery.

The following subsections start with a description of the original mvMDE algorithm, continue with the introduction of the SmvMDE variations and the changes they introduce to the mvMDE, and describe the experiments conducted with synthetic and physiological time-series to analyse and benchmark their operation.

B. Multivariate Multiscale Dispersion Entropy

DisEn arises from the integration of Shannon Entropy with symbolic dynamics, aiming to quantify the degree of irregularity in an input time-series segment. It achieves good discrimination capacity between different types of physiological activity while maintaining a low computational time [26], [27]. Multivariate Multiscale Dispersion Entropy (mvMDE) allows the multivariate quantification of DisEn from multi-channel time-series taking into consideration both temporal and spatial dynamics, across multiple time scales. The variation of the mvMDE algorithm which is used as the foundation for this study is the fourth and recommended by its designers, variation presented in the original study [34].

1) Coarse-Graining Process for Multiscale Implementation:

For the successful quantification of a time-series' complexity across multiple time scales, a number of coarse graining procedures have been suggested as a preprocessing step

of the entropy quantification algorithms. These include the widely used moving average approach [47]–[49], the low-pass Butterworth filtering [49], [50], and the empirical mode decomposition [50]. This study builds upon the original algorithmic implementation of mvMDE and therefore utilizes the moving average coarse graining approach for simplicity [34], although other alternatives provide better frequency responses. Based on this approach, in a set of p -channel time-series $\mathbf{Y} = \{y_{k,b}\}_{k=1,2,\dots,p}^{b=1,2,\dots,N}$ each channel is processed separately and divided into non-overlapping segments of length equal to the defined time scale factor τ . For each segment, an average value is calculated and used to derive the coarse-grained multi channel time-series as follows:

$$x_{k,i}(\tau) = \frac{1}{\tau} \sum_{b=(i-1)\tau+1}^{i\tau} y_{k,b}, 1 \leq i \leq \left\lfloor \frac{L}{\tau} \right\rfloor = N, 1 \leq k \leq p \quad (1)$$

where L is the original channel length and N the resulting coarse-grained channel length.

2) Application of Mapping Function: For the implementation of mvMDE, a recommended step is the application of a non-linear mapping function to each channel, such as the normal cumulative distribution function (NCDF) [34]. The selection of a non-linear over a linear mapping function is made to ensure that maximum and minimum amplitude values that can be significantly larger or smaller than the mean value of the channel do not disrupt the initial step of allocating samples to classes by forcing the majority of samples to be allocated to a small number of classes [26], [27], [51]. For multiscale implementations using NCDF the mean and standard deviation (σ) of the original non coarse-grained time-series are used and remain constant for the mapping process across all temporal scale factors. This ensures that the mapping based on the NCDF remains fixed and is not affected by the averaging taking place during the coarse graining process [34].

3) Algorithm for mvMDE: For a set of p -channel time-series $\mathbf{X} = \{x_{k,i}\}_{k=1,2,\dots,p}^{i=1,2,\dots,N}$ of length N each, the computational steps of mvMDE are the following [34]:

- 1) Production of univariate quantised time-series: A number of classes $(1, 2, \dots, c)$ are distributed along the amplitude range of each channel separately. Their samples are allocated to their nearest respective class based on their amplitude. As a result, a quantized channel $u_j(j = 1, 2, \dots, N)$ is produced for each respective input channel, resulting in a set of p -quantized channels $\mathbf{U} = \{u_{k,i}\}_{k=1,2,\dots,p}^{i=1,2,\dots,N}$.
- 2) Formulation of multivariate embedded vectors: From $\{u_{k,i}\}$, the quantized samples are embedded into univariate vectors of length m (with a time delay d) for each channel. The univariate embedded vectors are then combined in sets of p -synchronised vectors, one from each channel. The vectors within each synchronised set are serially concatenated for the production of a respective multivariate embedded vector $Z(j)$, of length $m \cdot p$, for each $j = 1, 2, \dots, N - (m - 1)d$.
- 3) Mapping to multiple dispersion patterns: In mvMDE, each embedded vector is mapped to multiple dispersion patterns to effectively evaluate patterns both temporally

within the same channel as well as across channels. Each subset of m elements in $Z(j)$ is accessed, following all possible $\binom{m \cdot p}{m}$ combinations. This formulates $\phi_q(j)(q = 1, \dots, \binom{m \cdot p}{m})$ subvectors, that are then mapped to their corresponding $\pi_{v_0 \dots v_{m-1}}$ dispersion pattern. As a result, the total number of dispersion pattern instances is $(N - (m - 1)d) \binom{m \cdot p}{m}$ and the number of unique dispersion patterns is c^m .

- 4) Calculation of Dispersion Pattern Relative Frequency: For each of the c^m unique dispersion patterns, their relative frequency is calculated as follows, with $\#$ being the symbol that signifies the cardinality of the set:

$$\frac{p(\pi_{v_0 \dots v_{m-1}}) = \# \{j | j \leq N - (m - 1)d, \phi_q(j) \text{ has type } \pi_{v_0 \dots v_{m-1}}\}}{(N - (m - 1)d) \binom{m \cdot p}{m}} \quad (2)$$

- 5) Calculation of Multivariate Dispersion Entropy: Utilizing the relative frequencies of the dispersion patterns computed as above considering both temporal and spatial domains, the DisEn value for \mathbf{X} is calculated based on Shannon's definition of entropy. The output DisEn is normalized in the range of 0 to 1 by dividing with $\log c^m$:

$$mvMDE(\mathbf{X}, m, c, d) = - \sum_{\pi=1}^{c^m} \frac{p(\pi_{v_0 \dots v_{m-1}}) \cdot \ln(p(\pi_{v_0 \dots v_{m-1}}))}{\ln c^m} \quad (3)$$

C. Stratified-Dispersion Entropy Variations

Building on the original mvMDE, we introduce three variations of SmvMDE as an initial implementation of the Stratified Entropy Framework. With their two strata configuration, the SmvMDE variations separate the channels in two sets. The set of one or more designated channels, which are allocated to the "core" stratum and the set of secondary channels which are allocated to the "periphery" stratum.

The original mvMDE treats all combinations for the multivariate embedded vectors as equal. Instead, the SmvMDE variations prioritise combinations that contain samples retrieved from designated channels. The Threshold (T-SmvMDE), Soft Threshold (ST-SmvMDE), and Proportional (P-SmvMDE) variations utilize distinct approaches for adjusting the contribution of each combination through the modification of the third and fourth steps of the original mvMDE algorithm, as described in subsection II-B.3. The code for the implementation of the SmvMDE variations using Matlab is publicly available at: <https://github.com/EvangelosKafantaris/SmvMDE.git>.

1) Threshold Variation: T-SmvMDE utilizes a new input parameter compared to the original mvMDE. The threshold parameter (t), which defines the minimum number of samples extracted from designated channels that each combination should contain in order to be utilized by the algorithm.

Consequently the initially $\binom{m \cdot p}{m}$ combinations utilized in the case of the original mvMDE are reduced to a subset of length l_t that only includes combinations that meet or surpass

the threshold of t samples. As a result, for each multivariate embedded vector $Z(j)$ only $\phi_q(j)(q = 1, \dots, l_t)$ subvectors are mapped to dispersion patterns. This results in the reduction of dispersion pattern instances to $(N - (m - 1)d)l_t$.

Hence, for each unique dispersion pattern, their relative frequency is calculated with a modified denominator to match the reduced number of dispersion patterns:

$$p(\pi_{v_0 \dots v_{m-1}}) = \frac{\#\{j \mid j \leq N - (m - 1)d, \phi_q(j) \text{ has type } \pi_{v_0 \dots v_{m-1}}\}}{(N - (m - 1)d)l_t} \quad (4)$$

2) Soft Threshold Variation: As an intermediate algorithm between T-SmvMDE and mvMDE, ST-SmvMDE combines the t input parameter with the additional reduced weight (w) parameter to reduce the contribution of combinations that do not meet the threshold of t , without removing them completely. The possible values of the w parameter range from a minimum value of 0, where the output entropy value will match that of T-SmvMDE, and a maximum value of 1, where the output entropy value will match that of the original mvMDE algorithm, since no reduction of contribution will occur.

Based on the t parameter, the combinations for the multivariate embedded vectors are split into two subsets: A primary subset of combinations with length l_p whose contribution to the calculation of a dispersion pattern's frequency remains unchanged; and the secondary subset with length l_s whose impact is reduced by multiplying the number of respective dispersion pattern instances with w . Consequently, for each $Z(j)$: $\phi_p(j)(p = 1, \dots, l_p)$ subvectors are formulated from the primary and $\phi_s(j)(s = 1, \dots, l_s)$ from the secondary subset, respectively.

Therefore, the maximum value of instances for a dispersion pattern becomes $(N - (m - 1)d)(l_p + (l_s w))$. As a result, for each unique dispersion pattern, their relative frequency is:

$$p(\pi_{v_0 \dots v_{m-1}}) = \frac{\#\{j \mid j \leq N - (m - 1)d, \phi_p(j) \text{ has type } \pi_{v_0 \dots v_{m-1}}\}}{(N - (m - 1)d)(l_p + l_s w)} + \frac{\#\{j \mid j \leq N - (m - 1)d, \phi_s(j) \text{ has type } \pi_{v_0 \dots v_{m-1}}\}}{(N - (m - 1)d)(l_p + l_s w)} \cdot w \quad (5)$$

3) Proportional Variation: The third variation, P-SmvMDE, requires no additional parameters. Instead of utilizing a threshold to filter combinations, it allocates them in subsets based on the number of samples contained in each combination that are retrieved from designated channels and applies a proportional factor to each category. With m being the length of the combination and h being the number of samples taken from designated channels, this factor is defined as $\frac{h}{m}$.

Therefore, the values of the proportional factor range from a minimum of 0 to a maximum of 1 and the total number of subsets in which the combinations are allocated is equal to $m + 1$. Consequently, for each $Z(j)$, $\phi_h(j)(h = 1, \dots, l_h)$ subvectors are formulated from each subset with l_h being the length of the respective subset. Hence, the maximum value of instances (α) for a dispersion pattern becomes $\alpha = \sum_{h=0}^m (N - (m - 1)d)(l_h \frac{h}{m})$.

TABLE I
PARAMETERS VALUES FOR SYNTHETIC TIME-SERIES (ST) AND
PHYSIOLOGICAL TIME-SERIES (PT) EXPERIMENTS

Parameter	Symbol	ST	RWD
Embedding Dimension	m	2	3
Number of classes	c	5	6
Time Delay	d	1	1
Scale Factor Range	τ	1 to 20	1 to 10
Threshold (T and ST CmvMDE)	t	1	1
Reduced Weight (ST CmvMDE)	w	0.5	0.5

The relative frequency of each unique dispersion pattern is calculated by counting dispersion pattern instances in combinations of each subset multiplied by their respective proportional ($\frac{h}{m}$) factor, divided by the maximum value of instances:

$$p(\pi_{v_0 \dots v_{m-1}}) = \frac{1}{\alpha} \cdot \sum_{h=0}^m \#\{j \mid j \leq N - (m - 1)d, \phi_h(j) \text{ has type } \pi_{v_0 \dots v_{m-1}}\} \cdot \frac{h}{m} \quad (6)$$

D. Synthetic Time-Series Experiments

1) Uncorrelated white Gaussian and 1/f noise: To compare the operation of the SmvMDE variations and the original mvMDE across multiple scales we utilize combinations of uncorrelated white Gaussian noise (WGN) and 1/f noise due to their differences in complexity and irregularity. Complexity in a time-series arises from consistent structural dynamics and therefore, when measured, is expected to follow a stable multiscale profile [47], [52]. Irregularity consists of random fluctuations that do not arise from underlying structural dynamics and is expected to have an inconsistent multiscale profile. The complexity of 1/f noise is higher than WGN while the irregularity of WGN is higher than 1/f [36], [53]. Thus, multivariate combinations of WGN and 1/f time-series have been used in previous research to test the multiscale operation of entropy quantification algorithms, with the complexity of 1/f leading to a stable output entropy value across increasing time scales while the entropy values of WGN decrease with time scale [54], [55].

2) Formulation of Experimental Setups: To test the operation of mvMDE and SmvMDE, all possible combinations of WGN and 1/f noise are formulated in 3-channel time-series, resulting in the following inputs for the experiments:

- 1) Three WGN channels.
- 2) Two WGN and one 1/f channels.
- 3) One WGN and two 1/f channels.
- 4) Three 1/f channels.

Considering the operation of SmvMDE, the output entropy value is expected to be affected to a larger degree by any designated channel allocated to the core stratum over those allocated to the periphery stratum. This would not affect experimental setups 1) and 4) which contain homogeneous channels of only WGN or only 1/f noise. However, it would lead to different results for experimental setups 2) and 3) which contain both

WGN and $1/f$ channels based on their allocation to strata. Therefore, to study the operation of SmvMDE variations, experimental setups 2) and 3) are expanded. In a first iteration, the designated channel is one of the WGN channels, followed by a second iteration where the designated channel is one of the $1/f$ channels, to observe how the prioritization of each type of channel affects the output. This results in a total of six experimental setups for SmvMDE:

- 1) Three WGN channels.
- 2) Two WGN and one $1/f$ channels with WGN designated.
- 3) One WGN and two $1/f$ channels with WGN designated.
- 4) Two WGN and one $1/f$ channels with $1/f$ designated.
- 5) One WGN and two $1/f$ channels with $1/f$ designated.
- 6) Three $1/f$ channels.

3) Statistical Analysis: Each experimental setup is repeated 40 times independently and the respective mean and σ are calculated for each τ value from 1 to 10. Finally, all experimental setups are replicated for channel lengths of 15,000 and 300 samples to assess potential differences between the analysis of long versus short time-series. The results are reported separately for each algorithm and experimental setup. The parameter values used for mvMDE and SmvMDE are chosen based on the limitations introduced by the short length time-series and are matching those used in the original mvMDE study to allow comparison between the two studies [34]. They are displayed in Table I under the Synthetic Time-Series (ST) column.

4) Computational Time Experiments: To ensure that SmvMDE variations maintain the low computation time properties of the original mvMDE, 2-channel, 5-channel and 8-channel time-series are formulated from uncorrelated WGN with channel lengths ranging from 1000 up to 100,000 samples. Each experimental setup is repeated over 20 independent realizations and the average computation time is calculated and reported for the mvMDE and SmvMDE algorithms. For the implementation of SmvMDE algorithms, an arbitrary designated channel is selected. The computations are carried out using a PC with Intel(R) Core(TM) i7-8750H CPU @ 2.2 GHZ, 16 GB RAM running MATLAB R2018b. The parameter values of mvMDE and SmvMDE remain the same with the exception of τ_{max} being reduced from 20 to 10 to be consistent with prior research [34].

E. Physiological Time-Series Experiments

1) MIT-BIH Polysomnographic Database: To test the operation of the algorithms on multi-channel time-series formulated from signals extracted from different organ systems, the publicly available MIT-BIH Polysomnographic Database is utilized which contains a total of 18 records of multiple physiological signals initially recorded for the evaluation of chronic obstructive sleep apnea (OSA) syndrome and digitized at a sampling rate of 250 Hz [56], [57].

For the purpose of this study the records slp41 and slp45 are selected, due to the availability of extensive sections of healthy stage 2 sleep and the records slp04, slp16 due to the existence of multiple incidents of obstructive apnea with arousal that occurred during stage 2 sleep. All four records

contain complete and synchronized recordings of EEG, ECG, BP and RESP signals. The EEG signal is split into the frequency bands of: delta (0.5 - 3.5 Hz), theta (4 - 7.5 Hz), alpha (8 - 11.5 Hz), sigma (12 - 15.5 Hz) and beta (16 - 19.5 Hz) [58]. Hence from each record, 8-channel time-series are extracted consisting of the channels: Delta, Theta, Alpha, Sigma, Beta, ECG, BP and RESP channels.

2) Formulation and Selection of Analysis Windows: These time-series are split into 8-channel non-overlapping windows with 7,500 samples per channel corresponding to the 30 second annotation intervals of the database. Based on the target annotation for each record, 235 multi-channel "healthy" windows are selected and extracted corresponding to healthy stage 2 sleep (slp41 = 96 windows, slp45 = 139 windows) and 235 multi-channel "apnea" windows corresponding to OSA with arousal during stage 2 sleep (slp04 = 140 windows, slp16 = 95 windows). As a result, a "healthy" and an "apnea" dataset are formulated consisting of 235 windows each.

3) Calculation of DisEn: The parameter values for the extraction of multiscale entropy distributions from the 235 "healthy" and 235 "apnea" windows are chosen based on the considerations discussed in subsection III-D. The values are displayed in Table I under the physiological time-series (PT) column. Each distribution extracted per window contains ten values, one for each τ value from 1 to 10.

For the mvMDE algorithm one multiscale distribution is extracted from the "healthy" dataset and a second one from the "apnea" one. For the effective study of SmvMDE variations (T, ST, and P), the variations are applied in a total of eight iterations for each dataset. During each iteration a different channel is designated. This leads to the extraction of eight multiscale distributions from each dataset, for a total of 16, to study how the prioritization of each channel's dynamics affects the output entropy values and the physiological differentiation capacity of SmvMDE.

4) Statistical Analysis: To effectively measure and benchmark the differentiation capacity of SmvMDE variations to mvMDE, the following steps have to be completed for each τ value separately:

- 1) The computation of Hedges' g effect size [59] for the "healthy" versus "apnea" output distributions using a non-parametric Permutation test [60].
- 2) For each SmvMDE variation and designated channel selection, the calculation of effect size difference when moving from mvMDE to the respective SmvMDE variation.
- 3) The estimation of confidence intervals for each effect size difference calculated when moving from mvMDE to one of the SmvMDE variations to verify their significance.

As a prerequisite step for the estimation of confidence intervals, bootstrapping is applied to the distributions extracted from the "healthy" and "apnea" datasets. The bootstrapping is implemented by sampling with replacement the sets of 235 multiscale values within each output distribution. In total, for each of the 16 distributions per SmvMDE variation, 40 independent realizations of bootstrapped distributions are generated. No bootstrapping is applied to the two output distribu-

tions of mvMDE. This is to ensure that SmvMDE distributions are benchmarked to the same mvMDE distributions.

To successfully implement the aforementioned analysis, the bootstrapped distributions of each SmvMDE and the original distributions of mvMDE are utilized in the following computation steps applied for each designated channel selection and at each τ value from 1 to 10:

- 1) Each of the 40 bootstrapped "healthy" distributions are paired at random with one of the 40 bootstrapped "apnea" distributions. The pairing is kept the same across all SmvMDE variations for consistency.
- 2) Between the two distributions of each pair a non-parametric Permutation Test with 100,000 permutations is applied. These results in the extraction of a total of 40 multiscale sets of Hedges' g effect size values.
- 3) The same process takes place once, between the two distributions of mvMDE resulting in Hedges' g effect size values.
- 4) The benchmarking effect size values of mvMDE are subtracted from the effect size values extracted from each pair of bootstrapped distributions. This results in a total of 40 multiscale sets of effect size differences.
- 5) Finally, the mean of the 40 effect size differences and the 95% confidence intervals are calculated.

The results of the Statistical Analysis for an SmvMDE variation are visualized by plotting, for each designated channel, the mean and 95% confidence intervals of the effect size difference at each τ value from 1 to 10.

III. RESULTS AND DISCUSSION

A. Synthetic Time-Series Experiments

The results of the application of mvMDE and SmvMDE on 3-channel time-series of WGN and $1/f$ noise, are presented in Figures 1 for univariate length of 15,000 samples and in Figures 2 for univariate length of 300 samples. Each experimental setup is replicated for 40 independent iterations and the mean and σ of DisEn values are plotted in the respective figures for each value of τ from 1 to 20.

1) *mvMDE Operation*: The operation of the mvMDE matches the patterns that have been verified by prior research [34]. As τ increases, the output entropy value has a stronger decline for the 3-channel WGN time-series. As the number of $1/f$ channels increase, the output entropy value follows a more stable profile with the 3-channel $1/f$ time-series being the most stable.

2) *SmvMDE Operation*: For experimental setups 1 and 6 that contain solely WGN channels and $1/f$ channels respectively, the operation of all three SmvMDE variations is identical to the mvMDE, as expected. Contrariwise, experiments 2 to 5 follow the pattern of prioritizing the characteristics of the designated channel. When a WGN channel is designated, a stronger decline of output entropy is observed as τ increases, while when a $1/f$ channel is designated the output follows a more stable profile for increasing values of τ .

When comparing the results of the three SmvMDE variations for the same experimental setup:

TABLE II
COMPUTATIONAL TIME OF mvMDE AND SmvMDE IN SECONDS

Samples and Channels	mvMDE	T	ST	P
1,000 samples and 2-channels	0.024	0.025	0.026	0.026
1,000 samples and 5-channels	0.061	0.059	0.064	0.065
1,000 samples and 8-channels	0.100	0.0095	0.117	0.126
3,000 samples and 2-channels	0.067	0.069	0.069	0.070
3,000 samples and 5-channels	0.177	0.171	0.183	0.187
3,000 samples and 8-channels	0.302	0.285	0.339	0.356
10,000 samples and 2-channels	0.241	0.251	0.250	0.255
10,000 samples and 5-channels	0.649	0.631	0.663	0.685
10,000 samples and 8-channels	1.182	1.029	1.240	1.254
30,000 samples and 2-channels	1.056	1.091	1.101	1.108
30,000 samples and 5-channels	2.839	2.612	2.879	2.870
30,000 samples and 8-channels	4.789	4.526	5.044	5.044
100,000 samples and 2-channels	8.048	8.067	8.202	8.181
100,000 samples and 5-channels	20.550	20.157	20.820	20.967
100,000 samples and 8-channels	33.571	32.436	35.243	35.133

- 1) Using the mvMDE output values as reference, the largest deviations are observed by the P-SmvMDE variation, followed by the T-SmvMDE, and then the ST-SmvMDE variation.
- 2) The ST-SmvMDE outputs are between those of T-SmvMDE and mvMDE as expected by its design and the selected parameter values, with the w value set to 0.5.
- 3) The higher deviation of the P-SmvMDE outputs from mvMDE is expected when considering that for an $m = 2$ the P-SmvMDE variation gives a higher prioritization to the core stratum than the respective implementation of T-SmvMDE with $m = 2$ and $t = 1$.

3) *Short Length Time-Series*: Figure 2 display the results for the 300 sample length experiments. For all tested algorithms, the outputs follow the same patterns as their 15,000 sample length equivalent indicating that the operation of SmvMDE variations remains the same regardless of time-series length. However, for all experimental setups, the σ values are increased, with the increase being stronger for higher τ values, as expected due to the short time-series length. Consequently, between the outputs of SmvMDE variations, overlapping can be observed between the experimental setups 2 to 5. This indicates that during the analysis of multi-channel time-series, the sample size of the window being analyzed should be larger than the respective minimum size for mvMDE for prioritization of the core stratum to be noticeable.

B. Computation Time Benchmarks

The results in Table II indicate that SmvMDE variations maintain the low computation time of the original mvMDE, as expected, since no computationally critical operations have been modified and the linear time complexity is maintained. Across all variations the main factor affecting the overall computation time is the univariate length of the time-series. When comparing the results for experimental setups with the same univariate length, the differences in computation time between the original mvMDE and the SmvMDE variations become more noticeable for higher number of channels.

The maximum differences in computation time are noted in the experimental setup with a univariate time-series length

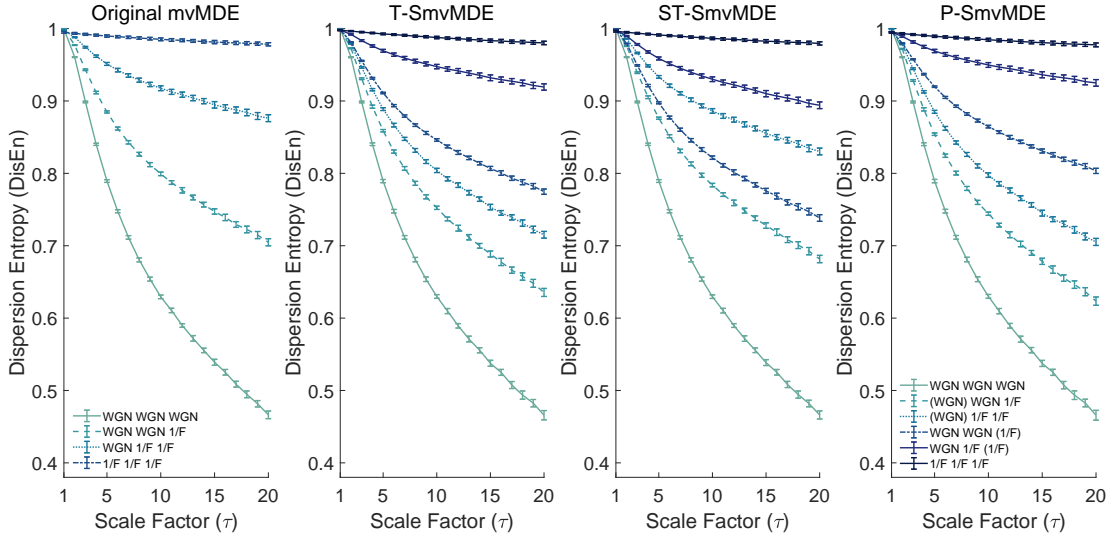


Fig. 1. The mean and σ of output DisEn are plotted for τ values of 1 to 20 for the four experimental setups of mvMDE and the six experimental setups of SmvMDE with time-series length of 15,000 samples. For SmvMDE, the designated channel is displayed within ().

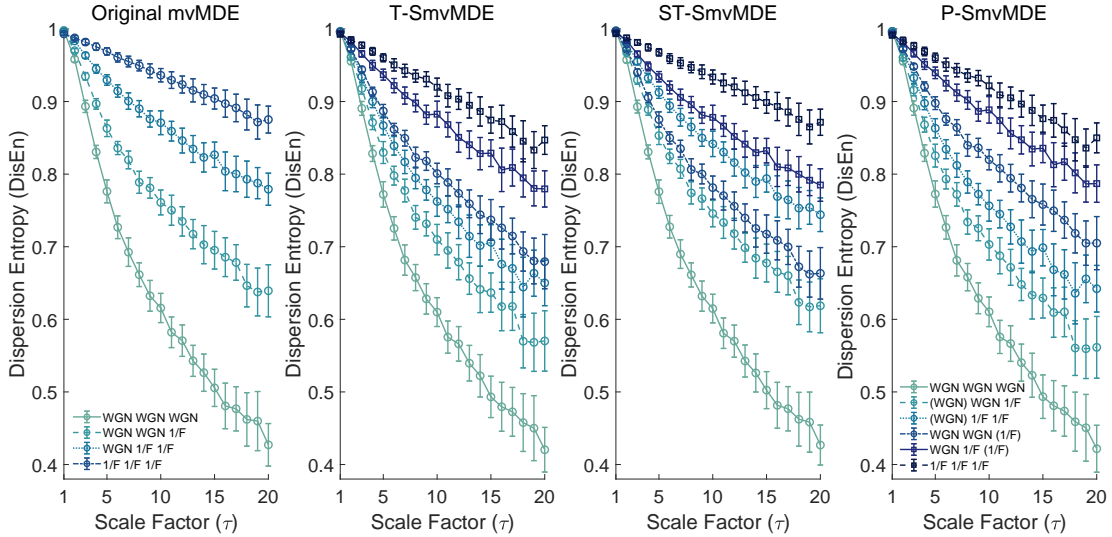


Fig. 2. The mean and σ of output DisEn are plotted for τ values of 1 to 20 for the four experimental setups of mvMDE and the six experimental setups of SmvMDE with time-series length of 300 samples. For SmvMDE, the designated channel is displayed within ().

of 100,000 samples and 8-channels. The maximum increase of 1.672 seconds (4.98%) is noted when moving from the mvMDE to the ST-SmvMDE algorithm while the maximum decrease of 1.135 seconds (3.38%) is noted when moving from mvMDE to T-SmvMDE. The decrease of computation time in the case of T-SmvMDE is an expected benefit due to the lower number of combinations utilised in that variation.

C. Physiological Time-Series Experiments

The results of the statistical analysis implemented on the output entropy distributions extracted from the application of the mvMDE and SmvMDE algorithms on the 235 "healthy" and 235 "apnea" 8-channel windows are presented in Figure 3.

In this subsection only the T-SmvMDE and P-SmvMDE results are reported and discussed in detail. As shown in

subsection II-C.2, ST-SmvMDE is by design an intermediary variation between T-SmvMDE and mvMDE. As a result, its outputs also follow an intermediary pattern which would be closer to the operation of mvMDE leading to smaller effect size differences.

1) T-SmvMDE Operation: Fig. 3 presents the results of the analysis measuring the effect size difference when moving from mvMDE to T-SmvMDE and P-SmvMDE for each designated channel selection. The mean Hedges' g effect size difference and the 95% confidence intervals are plotted for each τ value in the range of 1 to 10. For clarity, only the confidence intervals that do not cross the effect size difference axis at 0 are plotted.

The benchmarking of T-SmvMDE indicates that the prioritization of the following channels leads to consistent increases in differences between the output entropy distributions

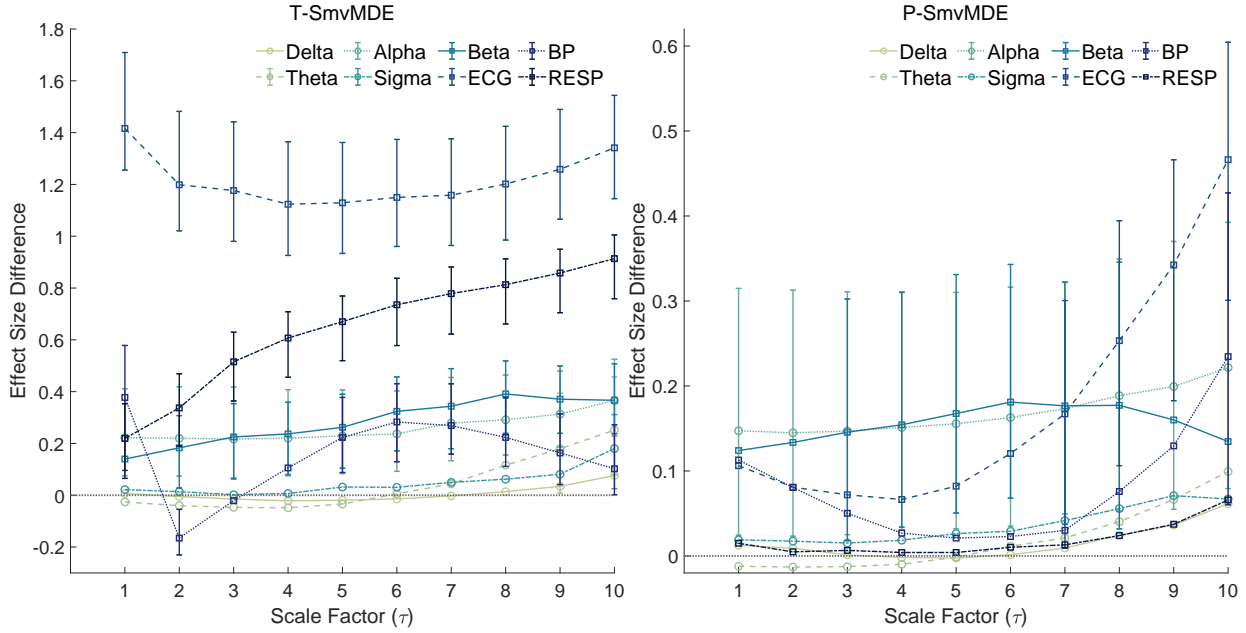


Fig. 3. The mean and the 95% confidence intervals of the effect size difference calculated from subtracting the multiscale mvMDE Hedges' g effect sizes from those of T-SmvMDE (left plot) and P-SmvMDE (right plot) are displayed for each designated channel selection.

extracted from "healthy" vs "apnea" windows when moving from the application of mvMDE to T-SmvMDE:

- ECG, RESP, and Alpha channels across all values of τ .
- Beta for τ values of 2 to 10.
- BP for τ values of 5 to 10.

The multiple cases of increases in effect size indicate that the T-SmvMDE variation might be quantifying differences between the two distributions that the direct application of mvMDE was not able to highlight during the analysis of the respective windows.

2) *P-SmvMDE Operation*: The respective benchmarking results for P-SmvMDE indicate that increases in differences between the output entropy distributions are observed when prioritizing one of the following channels.

- Alpha across all values of τ .
- Beta for τ values of 3 to 8.
- ECG for τ 7 to 10.

It is important to note that the designated channels displaying increased discrimination capacity for P-SmvMDE were also highlighted by T-SmvMDE. However, the increases observed by moving to P-SmvMDE were smaller in magnitude and were observed for fewer channels being prioritized when compared to T-SmvMDE. Considering the parameter values used for the SmvMDE variations in this setup, the T-SmvMDE set a higher prioritization to the core stratum over the periphery when compared to P-SmvMDE. Following the presented results, this may indicate that the particular application benefited from algorithmic implementations that defined stronger prioritization.

Furthermore, within the framework of Stratified Entropy, the detection of certain prioritization cases as being more effective in extracting distinct feature distributions between physiological states highlights the potential for the develop-

ment of feature selection methodologies that would aim to optimize physiological classification tasks.

D. On the implementation of Stratified Entropy

1) *Input Window Length*: For the implementation of entropy quantification, the selection of c and m parameter values defines the minimum univariate length of each channel within the input window. The univariate DisEn algorithm was capable of analysing short-length time-series [27] with minimum length (L) being $L > c^m \cdot \tau_{max}$. The mvMDE variation of the algorithm further improved its capacity to operate on short-length time-series due to the utilization of multivariate embedding vectors of increased length compared to their univariate counterparts [34] leading to a minimum length of: $L > \frac{c^m \cdot \tau_{max}}{\binom{m-p}{m}}$. In the case of SmvMDE variations, the minimum input length is between the limits of univariate DisEn and mvMDE. As shown in subsection III-A, overlapping was observed in the short-length time-series among the high τ value outputs while analyzing the same time-series with different channels being prioritized. Consequently, we would recommend the utilization of a stricter minimum, closer to the univariate DisEn: $L > c^m \cdot \tau_{max}$ when deploying SmvMDE variations to ensure that the effects of strata prioritization are quantifiable.

2) *Number of designated channels*: With m being an exponent in defining the minimum input window length, it is important to consider that during the implementation of Stratified Entropy, an increased value of m might be needed when increasing the number of designated channels. In this case it is important ensure that there are not multiple combinations consisting entirely of samples retrieved from designated channels which would lead to them being treated equally and result to an output profile that would more strongly resemble

that of mvMDE. Furthermore, while an increase in the value of m would allow the allocation of additional designated channels this might not be an optimal approach since an overshadowing of dynamics would now be possible to occur within core stratum itself. For this reason we recommend that the majority of Stratified Entropy applications follow a conservative approach when allocating channels to the core stratum and instead utilize multiple iterations to extract features using different designated channels.

3) Number of Strata: The total number of strata defined in a Stratified Entropy implementation is a decision that has to be made prior to the design of a respective algorithm. It affects both the design and the implementation of the algorithm since appropriate algorithmic steps have to be formulated for the prioritization of channels based on their strata allocation, while the selection of appropriate parameter values is required for effective operation.

As an example, in the case of expanding the presented SmvMDE variations from a two to a three strata configuration, the T-SmvMDE and the ST-SmvMDE variations could be modified to operate with two different t and w (in the case of ST) values based on which strata are prioritized, while P-SmvMDE could be modified with having two tiers of proportional factors respectively. This design modification could be complemented with an appropriate increase of the m value to allow for samples of varied prioritization to be included in the same combinations similarly to the process discussed for having multiple designated channels.

However, while the expansion of the total number of strata is possible, it increases algorithmic complexity and restricts the range of effective parameter values, particularly m as discussed above. Therefore configurations with increased numbers of strata might be more relevant for applications that would benefit from their utilization despite the increased complexity, such as for example when a priori knowledge exists with regards to the hierarchy of channels.

E. Limitations and Future Work

Our algorithmic variations display examples of successful implementations of the Stratified Entropy framework, with effective prioritization of the channels allocated to the core stratum over the periphery and the extraction of novel features. However, it is important to expand its implementation using additional entropy quantification algorithms, such as PEn to which our framework is directly applicable, to acquire a more complete perspective on the utility that the framework offers. Furthermore, due to its capacity to be applied in a modular manner and with low computational cost, it would be worthwhile to combine Stratified Entropy with other variations of entropy algorithms to target specific applications. Examples include its integration with the aforementioned non-uniform multiscale embedding to incorporate a priori knowledge, with optimal scale selection for each channel, or the utilization of a fuzzy membership function in DisEn [61].

Finally, while the presented study indicates that the resulting feature distributions extracted via SmvMDE can display increased differences when comparing between healthy and

pathological physiological states, the use of machine learning with feature selection could provide further insights with regards to the benefits of SmvMDE for physiological state classification and prediction.

IV. CONCLUSION

This study introduces the framework of Stratified Entropy and presents three algorithmic variations for its implementation. Stratified Entropy allows the extraction of features that would not be accessible through traditional multivariate analysis by allowing the prioritization of certain channels' dynamics over others' based on the allocation of channels to different strata. The SmvMDE variations extend the established mvMDE through the inclusion of algorithmic steps that prioritize samples extracted from channels in the prioritized core stratum during the calculation of the output entropy value.

The results from the application of SmvMDE to time-series consisting of uncorrelated WGN and $1/f$ noise indicate that the variations successfully prioritize the dynamics of the designated channel in accordance with their distinct algorithmic operations. The low computation time profile of the original mvMDE variation is maintained due to no computationally critical steps being modified. When applying the SmvMDE variations to 8-channel time-series formulated from different physiological signals, certain of the SmvMDE features produce distributions with higher statistical difference when comparing healthy versus OSA sleep of stage 2, indicating the potentially increased discrimination capacity of SmvMDE over mvMDE for applications that would benefit from a stratification of the time-series' channels.

The presented framework is flexible with regards to the number of channels allocated to the prioritized stratum and the total number of strata. Furthermore, it can be extended to additional entropy quantification algorithms and combined with machine learning. However, appropriate care should be taken when configuring the respective algorithms to ensure that they are effectively designed and implemented in terms of their algorithmic steps and the selected parameter values.

ACKNOWLEDGMENT

We would like to thank John Fabila Carrasco for his suggestions on the mathematical notations for SmvMDE algorithms and Ian Piper for our discussions with regards to the analysis of physiological time-series.

REFERENCES

- [1] A. K. Yetisen, J. L. Martinez-Hurtado, B. Ünal, A. Khademhosseini, and H. Butt, "Wearables in Medicine," *Advanced Materials*, vol. 30, no. 33, p. 1706910, Aug. 2018.
- [2] D. R. Witt, R. A. Kellogg, M. P. Snyder, and J. Dunn, "Windows into human health through wearables data analytics," *Current Opinion in Biomedical Engineering*, vol. 9, pp. 28–46, Mar. 2019.
- [3] C. W. Paine, V. V. Goel, E. Ely, C. D. Stave, S. Stemler, M. Zander, and C. P. Bonafide, "Systematic Review of Physiologic Monitor Alarm Characteristics and Pragmatic Interventions to Reduce Alarm Frequency: Review of Physiologic Monitor Alarms," *Journal of Hospital Medicine*, vol. 11, no. 2, pp. 136–144, Feb. 2016.
- [4] S. Cerutti, "Multivariate and multiscale analysis of biomedical signals: Towards a comprehensive approach to medical diagnosis," in *2012 25th IEEE International Symposium on Computer-Based Medical Systems (CBMS)*. Rome, Italy: IEEE, Jun. 2012, pp. 1–5.

- [5] E. Pereda, R. Q. Quiroga, and J. Bhattacharya, "Nonlinear multivariate analysis of neurophysiological signals," *Progress in Neurobiology*, vol. 77, no. 1-2, pp. 1-37, Sep. 2005.
- [6] S. Cerutti, D. Hoyer, and A. Voss, "Multiscale, multiorgan and multivariate complexity analyses of cardiovascular regulation," *Philosophical Transactions of the Royal Society A: Mathematical, Physical and Engineering Sciences*, vol. 367, no. 1892, pp. 1337-1358, Apr. 2009.
- [7] R. P. Bartsch, K. K. L. Liu, A. Bashan, and P. C. Ivanov, "Network Physiology: How Organ Systems Dynamically Interact," *PLOS ONE*, vol. 10, no. 11, p. e0142143, Nov. 2015.
- [8] R. Fossion, A. L. Rivera, and B. Estañol, "A physicist's view of homeostasis: how time series of continuous monitoring reflect the function of physiological variables in regulatory mechanisms," *Physiological Measurement*, vol. 39, no. 8, p. 084007, Aug. 2018.
- [9] A. L. Goldberger, L. A. N. Amaral, J. M. Hausdorff, P. C. Ivanov, C.-K. Peng, and H. E. Stanley, "Fractal dynamics in physiology: Alterations with disease and aging," *Proceedings of the National Academy of Sciences*, vol. 99, no. Supplement 1, pp. 2466-2472, Feb. 2002.
- [10] A. L. Goldberger, C.-K. Peng, and L. A. Lipsitz, "What is physiologic complexity and how does it change with aging and disease?" *Neurobiology of Aging*, vol. 23, no. 1, pp. 23-26, Jan. 2002.
- [11] N. Scafetta, R. E. Moon, and B. J. West, "Fractal response of physiological signals to stress conditions, environmental changes, and neurodegenerative diseases," *Complexity*, vol. 12, no. 5, pp. 12-17, May 2007.
- [12] R. J. Martis, U. R. Acharya, A. K. Ray, and C. Chakraborty, "Application of higher order cumulants to ECG signals for the cardiac health diagnosis," in *2011 Annual International Conference of the IEEE Engineering in Medicine and Biology Society*. Boston, MA: IEEE, Aug. 2011, pp. 1697-1700.
- [13] C. Pradhan, S. K. Jena, S. R. Nadar, and N. Pradhan, "Higher-Order Spectrum in Understanding Nonlinearity in EEG Rhythms," *Computational and Mathematical Methods in Medicine*, vol. 2012, pp. 1-8, 2012.
- [14] A. Müller, J. F. Kraemer, T. Penzel, H. Bonnemeier, J. Kurths, and N. Wessel, "Causality in physiological signals," *Physiological Measurement*, vol. 37, no. 5, pp. R46-R72, May 2016.
- [15] I. Azimi, T. Pahikkala, A. M. Rahmani, H. Niela-Vilén, A. Axelin, and P. Liljeberg, "Missing data resilient decision-making for healthcare IoT through personalization: A case study on maternal health," *Future Generation Computer Systems*, vol. 96, pp. 297-308, Jul. 2019.
- [16] R. B. Kumar, N. D. Goren, D. E. Stark, D. P. Wall, and C. A. Longhurst, "Automated integration of continuous glucose monitor data in the electronic health record using consumer technology," *Journal of the American Medical Informatics Association*, vol. 23, no. 3, pp. 532-537, May 2016.
- [17] G. B. Moody, "The PhysioNet/Computing in Cardiology Challenge 2010: Mind the Gap," *Comput Cardiol*, p. 13, 2010.
- [18] M. Ribeiro, T. Henriques, L. Castro, A. Souto, L. Antunes, C. Costa-Santos, and A. Teixeira, "The Entropy Universe," *Entropy*, vol. 23, no. 2, p. 222, Feb. 2021.
- [19] C. E. Shannon, "A Mathematical Theory of Communication," *Bell Syst. Tech. J.*, vol. 27, pp. 623-656, 1948.
- [20] A. Papoulis and S. U. Pillai, *Probability, random variables, and stochastic processes*, 4th ed. Boston: McGraw-Hill, 2002.
- [21] M. Rostaghi, M. R. Ashory, and H. Azami, "Application of dispersion entropy to status characterization of rotary machines," *Journal of Sound and Vibration*, vol. 438, pp. 291-308, Jan. 2019.
- [22] Z. Huo, M. Martinez-Garcia, Y. Zhang, R. Yan, and L. Shu, "Entropy Measures in Machine Fault Diagnosis: Insights and Applications," *IEEE Transactions on Instrumentation and Measurement*, vol. 69, no. 6, pp. 2607-2620, Jun. 2020.
- [23] Y. Wu, P. Shang, and Y. Li, "Modified generalized multiscale sample entropy and surrogate data analysis for financial time series," *Nonlinear Dynamics*, vol. 92, no. 3, pp. 1335-1350, May 2018.
- [24] Y. Zhang, P. Shang, and H. Xiong, "Multivariate generalized information entropy of financial time series," *Physica A: Statistical Mechanics and its Applications*, vol. 525, pp. 1212-1223, Jul. 2019.
- [25] C. Bandt and B. Pompe, "Permutation Entropy: A Natural Complexity Measure for Time Series," *Physical Review Letters*, vol. 88, no. 17, p. 174102, Apr. 2002.
- [26] M. Rostaghi and H. Azami, "Dispersion Entropy: A Measure for Time-Series Analysis," *IEEE Signal Processing Letters*, vol. 23, no. 5, pp. 610-614, May 2016.
- [27] H. Azami and J. Escudero, "Amplitude- and Fluctuation-Based Dispersion Entropy," *Entropy*, vol. 20, no. 3, p. 210, Mar. 2018.
- [28] E. Olofson, J. Sleight, and A. Dahan, "Permutation entropy of the electroencephalogram: a measure of anaesthetic drug effect," *British Journal of Anaesthesia*, vol. 101, no. 6, pp. 810-821, Dec. 2008.
- [29] S. M. Pincus, "Approximate entropy as a measure of system complexity," *Proceedings of the National Academy of Sciences*, vol. 88, no. 6, pp. 2297-2301, Mar. 1991.
- [30] D. Caldirola, L. Bellodi, A. Caumo, G. Migliarese, and G. Perna, "Approximate Entropy of Respiratory Patterns in Panic Disorder," *American Journal of Psychiatry*, vol. 161, no. 1, pp. 79-87, Jan. 2004.
- [31] J. S. Richman and J. R. Moorman, "Physiological time-series analysis using approximate entropy and sample entropy," *American Journal of Physiology-Heart and Circulatory Physiology*, vol. 278, no. 6, pp. H2039-H2049, Jun. 2000.
- [32] D. E. Lake, J. S. Richman, M. P. Griffin, and J. R. Moorman, "Sample entropy analysis of neonatal heart rate variability," *American Journal of Physiology-Regulatory, Integrative and Comparative Physiology*, vol. 283, no. 3, pp. R789-R797, Sep. 2002.
- [33] Weiting Chen, Zhizhong Wang, Hongbo Xie, and Wangxin Yu, "Characterization of Surface EMG Signal Based on Fuzzy Entropy," *IEEE Transactions on Neural Systems and Rehabilitation Engineering*, vol. 15, no. 2, pp. 266-272, Jun. 2007.
- [34] H. Azami, A. Fernández, and J. Escudero, "Multivariate Multiscale Dispersion Entropy of Biomedical Time Series," *Entropy*, vol. 21, no. 9, p. 913, Sep. 2019.
- [35] F. C. Morabito, D. Labate, F. La Foresta, A. Bramanti, G. Morabito, and I. Palamara, "Multivariate Multi-Scale Permutation Entropy for Complexity Analysis of Alzheimer's Disease EEG," *Entropy*, vol. 14, no. 7, pp. 1186-1202, Jul. 2012.
- [36] M. U. Ahmed and D. P. Mandic, "Multivariate multiscale entropy: A tool for complexity analysis of multichannel data," *Physical Review E*, vol. 84, no. 6, p. 061918, Dec. 2011.
- [37] H. Azami, K. Smith, and J. Escudero, "MEMD-enhanced multivariate fuzzy entropy for the evaluation of complexity in biomedical signals," in *2016 38th Annual International Conference of the IEEE Engineering in Medicine and Biology Society (EMBC)*. Orlando, FL, USA: IEEE, Aug. 2016, pp. 3761-3764.
- [38] S. Luo, "A review of electrocardiogram filtering," *Journal of Electrocardiology*, p. 11, 2010.
- [39] O. Dressler, G. Schneider, G. Stockmanns, and E. Kochs, "Awareness and the EEG power spectrum: analysis of frequencies," *British Journal of Anaesthesia*, vol. 93, no. 6, pp. 806-809, Dec. 2004.
- [40] H. M. Stauss, "Identification of blood pressure control mechanisms by power spectral analysis," *Clinical and Experimental Pharmacology and Physiology*, vol. 34, no. 4, pp. 362-368, Feb. 2007.
- [41] D. W. Kaczka, G. M. Barnas, B. Suki, and K. R. Lutchen, "Assessment of time-domain analyses for estimation of low-frequency respiratory mechanical properties and impedance spectra," *Annals of Biomedical Engineering*, vol. 23, no. 2, pp. 135-151, Mar. 1995.
- [42] B. Diong, H. Nazeran, P. Nava, and M. Goldman, "Modeling Human Respiratory Impedance," *IEEE Engineering in Medicine and Biology Magazine*, vol. 26, no. 1, pp. 48-55, Jan. 2007.
- [43] H. Gu and C.-A. Chou, "Optimizing non-uniform multivariate embedding for multiscale entropy analysis of complex systems," *Biomedical Signal Processing and Control*, vol. 71, p. 103206, Jan. 2022.
- [44] H. Xiao and D. P. Mandic, "Variational Embedding Multiscale Sample Entropy: A Tool for Complexity Analysis of Multichannel Systems," *Entropy*, vol. 24, no. 1, p. 26, Dec. 2021.
- [45] H.-B. Xie, Y.-P. Zheng, J.-Y. Guo, and X. Chen, "Cross-fuzzy entropy: A new method to test pattern synchrony of bivariate time series," *Information Sciences*, vol. 180, no. 9, pp. 1715-1724, May 2010.
- [46] W. Shi, P. Shang, and A. Lin, "The coupling analysis of stock market indices based on cross-permutation entropy," *Nonlinear Dynamics*, vol. 79, no. 4, pp. 2439-2447, Mar. 2015.
- [47] M. Costa, A. L. Goldberger, and C.-K. Peng, "Multiscale Entropy Analysis of Complex Physiologic Time Series," *Physical Review Letters*, vol. 89, no. 6, p. 068102, Jul. 2002.
- [48] M. U. Ahmed and D. P. Mandic, "Multivariate Multiscale Entropy Analysis," *IEEE Signal Processing Letters*, vol. 19, no. 2, pp. 91-94, Feb. 2012.
- [49] J. F. Valencia, A. Porta, M. Vallverdú, F. Claria, R. Baranowski, E. Orłowska-Baranowska, and P. Caminal, "Refined Multiscale Entropy: Application to 24-h Holter Recordings of Heart Period Variability in Healthy and Aortic Stenosis Subjects," *IEEE Transactions on Biomedical Engineering*, vol. 56, no. 9, pp. 2202-2213, Sep. 2009.
- [50] Hamed Azami and Javier Escudero, "Coarse-Graining Approaches in Univariate Multiscale Sample and Dispersion Entropy," *Entropy*, vol. 20, no. 2, p. 138, Feb. 2018.

- [51] E. Kafantaris, I. Piper, T.-Y. M. Lo, and J. Escudero, "Augmentation of Dispersion Entropy for Handling Missing and Outlier Samples in Physiological Signal Monitoring," *Entropy*, vol. 22, no. 3, p. 319, Mar. 2020.
- [52] M. Costa, A. L. Goldberger, and C.-K. Peng, "Multiscale entropy analysis of biological signals," *Physical Review E*, vol. 71, no. 2, Feb. 2005.
- [53] H. C. Fogedby, "On the phase space approach to complexity," *Journal of Statistical Physics*, vol. 69, no. 1-2, pp. 411–425, Oct. 1992.
- [54] H. Azami and J. Escudero, "Refined composite multivariate generalized multiscale fuzzy entropy: A tool for complexity analysis of multichannel signals," *Physica A: Statistical Mechanics and its Applications*, vol. 465, pp. 261–276, Jan. 2017.
- [55] A. Humeau-Heurtier, "Multivariate Generalized Multiscale Entropy Analysis," *Entropy*, vol. 18, no. 11, p. 411, Nov. 2016.
- [56] Y. Ichimaru and G. Moody, "Development of the polysomnographic database on CD-ROM," *Psychiatry and Clinical Neurosciences*, vol. 53, no. 2, pp. 175–177, Apr. 1999.
- [57] A. L. Goldberger, L. A. N. Amaral, L. Glass, J. M. Hausdorff, P. C. Ivanov, R. G. Mark, J. E. Mietus, G. B. Moody, C.-K. Peng, and H. E. Stanley, "PhysioBank, PhysioToolkit, and PhysioNet: Components of a New Research Resource for Complex Physiologic Signals," *Circulation*, vol. 101, no. 23, Jun. 2000.
- [58] A. Bashan, R. P. Bartsch, J. W. Kantelhardt, S. Havlin, and P. C. Ivanov, "Network physiology reveals relations between network topology and physiological function," *Nature Communications*, vol. 3, no. 1, Jan. 2012.
- [59] L. V. Hedges, "Distribution Theory for Glass's Estimator of Effect size and Related Estimators," *Journal of Educational Statistics*, vol. 6, no. 2, pp. 107–128, Jun. 1981.
- [60] L. R. Krol, "Permutation Test." [Online]. Available: <https://github.com/lrkrol/permutationTest>
- [61] M. Rostaghi, M. M. Khatibi, M. R. Ashory, and H. Azami, "Fuzzy Dispersion Entropy: A Nonlinear Measure for Signal Analysis," *IEEE Transactions on Fuzzy Systems*, pp. 1–1, 2021.

